Mon. Not. R. Astron. Soc. **000**, 1–?? () Printed 1 February 2008 (MN LaTeX style file v1.4)

The pair-wise velocity dispersion of galaxies: effects of non radial motions

A. Del Popolo

Dipartimento di Matematica, Università Statale di Bergamo, Piazza Rosate, 2 - I 24129 Bergamo, ITALY
Feza Gürsey Institute, P.O. Box 6 Çengelköy, Istanbul, Turkey
Boğaziçi University, 80185 Bebek, Istanbul, Turkey

ABSTRACT

I discuss the effect of non-radial motions on the small-scale pairwise peculiar velocity dispersions of galaxies (PVD) in a CDM model. I calculate the PVD for the SCDM model by means of the refined cosmic virial theorem (CVT) (Suto & Jing 1997 (hereafter SJ97)) and taking account of non-radial motions by means of Del Popolo & Gambera (1998) (hereafter DG98) model. I compare the results of the present model with the data from Davis & Peebles (1983), the IRAS value at $1h^{-1}$Mpc of Fisher et al. (1993) and Marzke et al. (1995). I show that while the SCDM model disagrees with the observed values, as pointed out by several authors (Peebles 1976, 1980; Davis & Peebles 1983 (hereafter DP83); Mo et. al 1993; Fisher et al. 1994b; SJ97; Jing et al. 1998 (hereafter J98)), taking account of non-radial motions produce smaller values for the PVD. At $r \leq 1h^{-1}$Mpc the result is in agreement with Bartlett & Blanchard (1996) (hereafter BB96). At the light of this last paper, the result may be also read as a strong dependence of the CVT prediction on the model chosen to describe the mass distribution around galaxies, suggesting that the CVT cannot be taken as a direct evidence of a low density universe. Similarly to what shown in Del Popolo & Gambera (1999, 2000) (hereafter DG99, DG00), Del Popolo et al. (1999) (hereafter D99), the agreement of our model to the observational data is due to a scale dependent bias induced by the presence of non-radial motions. Since the assumptions on which CVT is based have been questioned by several authors (BB96; SJ97), I also calculated the PVD using the redshift distortion in the redshift-space correlation function, $\xi_{\rm z}(r_{\rm p}, \pi)$, and I compared it with the PVD measured from the Las Campanas Redshift Survey by J98. The result confirms that non-radial motions influence the PVD making them better agree with observed data.

Key words: cosmology: theory - large scale structure of Universe - galaxies: formation

1 INTRODUCTION

The pairwise velocity dispersion of galaxies (PVD) is an important quantity that gives information on the structure and clustering of the universe. Peculiar velocities, originating from the action of gravitational fields, are a probe of the gravitational potentials produced by luminous and dark matter.

Several approaches have been developed to determine the PVD. In this paper, I'll be concerned with two of them, the first one based on the redshift-space distortions and the second one on the Cosmic Virial Theorem (hereafter CVT).

The first method relies on the fact that peculiar motions do not affect tangential distances, but only the radial ones. If we observe the three-dimensional distribution of galaxies in redshift-space, we can see that it is distorted with respect to that seen in real space: dense clusters appear elongated along the line of sight ('fingers of God' effect) and the correlation functions of galaxies are also distorted when they are viewed in redshift-space. The important point is that the redshift-space distortion effects can be used to get useful information on important quantities like the PVD. This can be done using the anisotropies created by the peculiar motions in the redshift space correlation function. From a redshift survey of galaxies, it is possible to measure the correlation function in redshift-space, $\xi(s)$. One can calculate $\xi(s)$ as function of the component of the separation

vector in the direction parallel (π) and perpendicular ($r_{\rm p}$) to the line of sight. Plotting the correlation function $\xi_{\rm z}(r_{\rm p}, \pi)$ in the π-$r_{\rm p}$ plane, redshift distortions give rise to:
1) a stretching of the contours of $\xi_{\rm z}(r_{\rm p}, \pi)$ along π on small scales (< a few Mpc) because of non-linear pairwise velocities;
2) a compression along the line of sight, π, on larger scales, because of bulk motions.
DP83 used the small scale distortion to get the PVD of galaxies, modelling the elongation of $\xi_{\rm z}(r_{\rm p}, \pi)$ along π as a convolution of the real-space correlation function with the distribution function $f(v_{12})$, being v_{12} the relative velocity of the galaxy pair in the direction of the line of sight. The quoted method, introduced by Davis et al. (1978), Peebles (1980), DP83 and Bean et al. (1983) has sometimes given discrepant values: DP83, using data from the CfA1, obtained a value of $\sigma_{12} = 340 \pm 40$km/s, at $r = 1h^{-1}$Mpc; Fisher et al. (1994a) using the IRAS 1.2 Jy survey, obtained a value of $\sigma_{12} = 317^{+40}_{-49}$km/s in agreement with that of DP83. Larger values was obtained by Marzke et al. (1995) using the CfA2 and the SSRS2 (Southern Sky Redshift Survey) redshift surveys, ($\sigma_{12} = 540 \pm 180$km/s), by Lin et al. (1995) ($\sigma_{12} = 452 \pm 60$km/s) using the Las Campanas Redshift Survey and by J98 ($\sigma_{12} = 570 \pm 80$km/s). Moreover, some authors (Mo et al. 1993; Marzke et al. 1995; Guzzo et al. 1997) have pointed out that the value of the PVD is very sensitive to the presence or absence of rich clusters in a sample. Other authors emphasized that being σ_{12} a pair-weighted statistic it is heavily weighted by the densest regions of a sample (Strauss 1997). In two recent papers, Sheth et al. (2000) and Jing et al. (2001) have shown that σ_{12} varies widely not only because of the previous effect, but also because of the morphological type of the galaxies entering the catalog. In particular, Sheth et al. (2000), showed that redshift space distorsions should affect red galaxies more strongly than blue. This result can partly explain the difference between the IRAS catalog σ_{12} and the σ_{12} computed from the more fair sample contained in the Las Campanas Redshift Survey (LCRS). However the most recent papers agree to values of the PVD in the range 400-600 km/s (J98). This final range of convergence of σ_{12}, although still large, comes because of the increasingly large volumes surveyed in the most recent work.

The σ_{12} statistics has been used as a discriminator of models. DP83's result compared with the SCDM model showed that the model predicts values of PVD larger than the observed ones and successive studies confirmed that the SCDM model disagrees with the observed values by a factor $3-6$ (Mo et al. 1993; Fisher et al. 1994b; Marzke et al. 1995). A new idea, that of biased galaxy formation (Kaiser 1984; Bardeen et al. 1986 (hereafter BBKS)), was needed to reduce the discrepancy between the SCDM model prediction and observations. Some recent studies have however shown that for the SCDM model the shape of the predicted PVD is different from that observed, since the SCDM model predicts a correlation function steeper than the observed one (J98). In any case, introducing a constant bias does not resolve the problem, and a scale-dependent bias is necessary to reduce the quoted discrepancy (J98).

Another tool that has long been used to determine σ_{12} is the Cosmic Virial Theorem (CVT) (Peebles 1976) relying on the assumption of hydrodynamic equilibrium of galaxies on small scales. Several authors (Fisher et al. 1994b; BB96; SJ97) have pointed out some limitations of the theorem. BB96 discussed how the mass distribution around a typical pair of galaxies affects the CVT predictions, while SJ97 improved the theorem taking into account the effect of the finite size of galaxies. These last authors showed that the CVT in its initial formulation overestimates the small-scale PVD.

In this paper, I'll study the effects of a non-local bias, induced by non-radial motions (see DG98, DG99, DG00; D99), on the PVD by means of both the CVT and the distortions in $\xi_z(r_{\rm p}, \pi)$.
The plan of the paper is the following: in section 2, I calculate the PVD using the CVT in the original form introduced by Peebles (1976) and the improved version of SJ97 and taking account of non-radial motions. The theoretical results are compared with observational data. In section 3, I calculate the PVD by means of the distortions in the redshift-space correlation function and compare the results with observations. Section 4 is devoted to conclusions.

2 PVD AND THE CVT

2.1 The CVT and the finite size of galaxies

The CVT introduced by Peebles (1976) is fundamentally an equation of hydrostatic equilibrium obtained assuming statistical equilibrium between galaxy pairs, on small scales. The formula describing this theorem, and giving the relative (one-dimensional) peculiar velocity dispersion as function of their separation r, can be obtained by means of the second BBGKY hierarchy equation. It can be expressed as:

$$\langle v_{12}^2(r)\rangle = \frac{6G\rho_{\rm b}}{\xi_\rho(r)}\int_r^\infty \frac{dr'}{r'}\int d\mathbf{z}\,\frac{\mathbf{r}'\cdot\mathbf{z}}{z^3}\zeta_\rho(r', z, |\mathbf{r}'-\mathbf{z}|), \tag{1}$$

where $\rho_{\rm b}$ is the mean density of the universe, ξ_ρ and ζ_ρ are the two and three-point correlation function of mass, respectively. Assuming the forms for the two and three-point correlation function of galaxies given by Groth & Peebles (1977) and DP83, namely:

$$\xi_{\rm g} = \left(\frac{r_0}{r}\right)^\gamma \tag{2}$$

[ht]

Figure 1. The threshold $\delta_{\rm c}$ as a function of the mass M, through the peak height ν, taking account of non-radial motions with the model of this paper (dashed line) is compared with the result of Sheth et al. (1999) (solid line), obtained using an ellipsoidal collapse model.

and

$$\zeta_{\rm g}(r_1, r_2, r_3) = Q_{\rm g}\left[\xi_{\rm g}(r_1)\xi_{\rm g}(r_2) + \xi_{\rm g}(r_2)\xi_{\rm g}(r_3) + \xi_{\rm g}(r_3)\xi_{\rm g}(r_1)\right] \tag{3}$$

where $Q_{\rm g} = 0.7 \pm 0.21$ (see BB96), $r_0 = (5.4 \pm 0.3)h^{-1}$Mpc, $\gamma = 1.77 \pm 0.04$, and assuming that the two and three-point correlation functions of mass, ξ_ρ and ζ_ρ follow the same scaling and satisfy the relations:

$$\xi_{\rm g}(r) = b^2\xi_\rho(r) \tag{4}$$

and

$$\zeta_{\rm g}(r_1, r_2, r_3) = Q_{\rm g}b^4\zeta_\rho(r_1, r_2, r_3)/Q_\rho \tag{5}$$

being b the bias parameter, the CVT gives (Peebles 1976; Suto 1993):

$$\langle v_{12}^2(r)\rangle^{1/2} = 1460\sqrt{\frac{\Omega_0 Q_\rho}{1.3b^2}}\sqrt{\frac{I_0(\gamma)}{33.2}}5.4^{\frac{\gamma-1.8}{2}}\left(\frac{r_0}{5.4h^{-1}{\rm Mpc}}\right)^{\frac{\gamma}{2}}\left(\frac{r}{1h^{-1}{\rm Mpc}}\right)^{\frac{2-\gamma}{2}} {\rm km/s} \tag{6}$$

where $I_0(\gamma)$ is a function given in Peebles (1980) (equation (75.12)) and Ω_0 is the density parameter. Numerical and analytical studies in non-linear gravitational clustering seem to indicate that Q_ρ can be approximated as a constant in the range $0.5 - 2$ (Suto 1996), which depends very weakly on the underlying cosmological model. We shall use the value 0.6, that gives the same predictions of BB96 uncorrected CVT (see their Fig. 1), which shall be used for comparisons with our paper (note that also a low value of this parameter gives prediction for the pairwise-peculiar velocity dispersions much larger than observations).

Equation (6) was improved by SJ97 by taking account of the fact that galaxies are not point-like, using perturbation analysis and numerical integration. They changed the CVT incorporating a non-zero core radius, $r_{\rm c}$, and softening the gravitational force by means of a Plummer law with softening radius $r_{\rm s}$ obtaining the final result:

$$\begin{aligned}\langle v_{12}^2(r)\rangle^{1/2} &= 1460\sqrt{\frac{\Omega_0 Q_\rho}{1.3b^2}}\, 5.4^{\frac{\gamma-1.8}{2}}\left(\frac{r_0}{5.4h^{-1}{\rm Mpc}}\right)^{\frac{\gamma}{2}} \\ &\times\sqrt{\frac{I(r_{\rm c}/r, r_{\rm s}/r; \gamma)}{33.2}}\left(\frac{r}{1h^{-1}{\rm Mpc}}\right)^{\frac{2-\gamma}{2}} {\rm km/s}\end{aligned} \tag{7}$$

[ht]

Figure 2. The bias factor $b(\nu)$ as function of ν^2. The solid line represents the spherical collapse prediction of Mo & White (1996), the dotted line the prediction for b obtained from the model of this paper and the dashed line the ellipsoidal collapse prediction of Sheth et al. (1999).

where $I(r_c/r, r_s/r; \gamma)$ is given in SJ97 (equation (10)). This result simply tells that by replacing $I_0(\gamma)$ with $I(r_c/r, r_s/r; \gamma)$ the finite size of the galaxies is automatically taken into account. Moreover they showed, using COBE normalized CDM models, that the quoted improvement of the CVT has as final result a reduction of the small-scale velocity dispersion of galaxies, but not enough to be in agreement with observations.

The final aim of this section is to determine the PVD, using the modified CVT and, moreover, taking into account non-radial motions.

2.2 The threshold δ_c, the selection function and bias

The goal quoted at the end of the previous subsection can be accomplished remembering that non-radial motions induce a non-local scale dependence of the bias parameter, b (see D99)) and taking into account this effect in equation (7).
In this subsection, we are going to show how to calculate the dependence of b on the peak height $\nu = \frac{\delta(0)}{\sigma}$, which is proportional, through the overdensity $\delta = \frac{\rho - \rho_b}{\rho_b}$ and σ, the rms value of δ, to the halo mass. The $b(\nu)$ dependence obtained shall be used in the next subsection to analyse the effects of non-radial motions on the PVD.

As shown by DG98, DG99, DG00, if non-radial motions are taken into account, the threshold δ_c is not a constant but is function of mass, M, (DG98, DG99, DG00):

$$\delta_c(\nu) = \delta_{co}\left[1 + \frac{8G^2}{\Omega_o^3 H_0^6 r_i^{10} \overline{\delta}(1+\overline{\delta})^3}\int_{a_{min}}^{a_{max}} \frac{L^2 \cdot da}{a^3}\right] \quad (8)$$

where $\delta_{co} = 1.68$ is the critical threshold for a spherical model, r_i is the initial radius, L the angular momentum, H_0 and Ω_0 the Hubble constant and the density parameter at the current epoch, respectively, a the expansion parameter and $\overline{\delta}$ the mean fractional density excess inside a shell of given radius and mass M. The mass dependence of the threshold parameter, $\delta_c(\nu)$, and the total specific angular momentum, $h(r,\nu) = L(r,\nu)/M$, acquired during expansion, were obtained in the same way as described in D99 (see also Fig. 1 of the quoted paper).
The result of the calculation is shown in Fig. 1, where I plot $\delta_c(\nu)$ obtained by means of the model of this paper together with that obtained by Sheth et al. (1999) using an ellipsoidal collapse model. The dashed line represents $\delta_c(\nu)$ obtained with the present model, while the solid line that of Sheth et al. (1999). Both models show that the threshold for collapse decreases with

mass. In other words, this means that, in order to form structure, more massive peaks must cross a lower threshold, $\delta_c(\nu)$, with respect to under-dense ones. At the same time, since the probability to find high peaks is larger in more dense regions, this means that, statistically, in order to form structure, peaks in more dense regions may have a lower value of the threshold, $\delta_c(\nu)$, with respect to those of under-dense regions. This is due to the fact that less massive objects are more influenced by external tides, and consequently they must be more overdense to collapse by a given time. In fact, the angular momentum acquired by a shell centred on a peak in the CDM density distribution is anti-correlated with density: high-density peaks acquire less angular momentum than low-density peaks (Hoffman 1986; Ryden 1988). A larger amount of angular momentum acquired by low-density peaks (with respect to the high-density ones) implies that these peaks can more easily resist gravitational collapse and consequently it is more difficult for them to form structure. This is in agreement with Audit et al. (1997), Peebles (1990) and DP98, which pointed out that the gravitational collapse is slowed down by the effect of the shear rather than fastened by it (as substained by other authors). Therefore, on small scales, where the shear is statistically greater, structures need, on average, a higher density contrast to collapse.

This results in a tendency for less dense regions to accrete less mass, with respect to a classical spherical model, inducing a *biasing* of over-dense regions towards higher mass. Moreover the scale dependence of the threshold, $\delta_c(\nu)$, implies also a scale dependence of the bias parameter, b, since the two parameters are connected (see Borgani 1990; Mo & White 1996; DG98, D99). In fact, according to the biased theory of galaxy formation, observable objects of mass $\simeq M$ arise from fluctuations of the density field, filtered on a scale $R_{\rm f}$, rising over a *global* threshold, $\delta > \delta_{\rm c} = \nu_t\sigma$, where σ is the rms value of δ and $\nu_{\rm t}$ is the threshold height. The number density of objects, $n_{\rm pk}$, that forms from peaks of density of height ν can be written, following BBKS, in the form:

$$n_{\rm pk} = \int_0^\infty t(\frac{\nu}{\nu_{\rm t}}) N_{pk}(\nu) d\nu \tag{9}$$

where $t(\frac{\nu}{\nu_{\rm t}})$ is the threshold function, and $N_{\rm pk}d\nu$ the differential number density of peaks (see BBKS - equation (4.3)). The threshold level $\nu_{\rm t}$ is defined so that the probability of a peak becoming an observable object is 1/2 when $\nu = \nu_{\rm t}$. In the sharp threshold case the selection function, is a Heaviside function $t(\frac{\nu}{\nu_{\rm t}}) = \theta(\nu - \nu_{\rm t})$. The threshold function is connected to the bias coefficient of a class of objects by (BBKS):

$$b(R_{\rm f}) = \frac{\langle\tilde{\nu}\rangle}{\sigma_o} + 1 \tag{10}$$

where $\langle\tilde{\nu}\rangle$ is:

$$\langle\tilde{\nu}\rangle = \int_0^\infty \left[\nu - \frac{\gamma\theta}{1-\gamma^2}\right] t(\frac{\nu}{\nu_{\rm t}}) N_{\rm pk}(\nu) d\nu \tag{11}$$

while, γ and ϑ are given in BBKS (respectively equation (4.6a); equation (6.14)).
The threshold (or selection) function can be obtained following the arguments given in Colafrancesco et al. (1995) and DG98. In this last paper the selection function is defined as:

$$t(\nu) = \int_{\delta_c}^\infty p\left[\overline{\delta}, \langle\overline{\delta}(r_{Mt}, \nu)\rangle, \sigma_{\overline{\delta}}(r_{Mt}, \nu)\right] d\delta \tag{12}$$

where $\overline{\delta}$ is the mean fractional density excess inside a given radius, as measured at the current epoch, assuming linear growth, $< \overline{\delta} >$ its average value (see Ryden & Gunn 1987) and $\sigma_{\overline{\delta}}$ its dispersion given in Lilje & Lahav (1991), and where the function

$$p\left[\overline{\delta}, \langle\overline{\delta}(r)\rangle\right] = \frac{1}{\sqrt{2\pi}\sigma_{\overline{\delta}}} \exp\left(-\frac{|\overline{\delta} - \langle\overline{\delta}(r)\rangle|^2}{2\sigma^2_{\overline{\delta}}}\right) \tag{13}$$

gives the probability that the peak overdensity, $\overline{\delta}$ is different from the average, in a Gaussian density field. The selection function depends on ν through the dependence of $\overline{\delta}(r)$ on ν. As displayed, the integrand is evaluated at a radius $r_{\rm Mt}$ which is the typical radius of the object that we are selecting. Moreover, the selection function $t(\nu)$ depends on the critical overdensity threshold for the collapse, $\delta_{\rm c}(\nu)$. Given $\delta_{\rm c}(\nu)$ and chosen a spectrum, the selection function is immediately obtained through equation (12) and equation (13). As shown in DG98 (see their Fig. 6), the selection function, as expected, differs from an Heaviside function (sharp threshold). The shape of the selection function depends on the values of the filtering length R_f and on non-radial motions. The value of ν at which the selection function $t(\nu)$ reaches the value 1 ($t(\nu) \simeq 1$) increases for growing values of the filtering radius, $R_{\rm f}$. This is due to the smoothing effect of the filtering process. The effect of non-radial motions is, firstly, that of shifting $t(\nu)$ towards higher values of ν, and, secondly, that of making it steeper.

This means that while in a θ threshold scheme, fluctuations below $\delta_{\rm c}(\nu)$ have zero probability to develop an observable object, and fluctuations above $\delta_{\rm c}(\nu)$ have zero probability not to develop an object, the situation is totally different when the threshold is not a sharp step function. In this case objects can also be formed from fluctuations below $\delta_{\rm c}(\nu)$ and there is a non-zero probability for fluctuations above $\delta_{\rm c}$ to be sterile. This result, in agreement with Borgani (1990), with the 'fuzzy'

threshold approach of Audit et al. (1997) and Sheth et al. (1999), is fundamentally connected to non-sphericity effects present during the gravitational growing process.

I want to remark that the choice made to calculate b, instead of the well known Mo & White (1996) model:

$$b = 1 + \frac{\nu^2 - 1}{\delta_c} \tag{14}$$

is motivated by the fact that I am interested in studying the PVD on scales $< 10h^{-1}$Mpc, while in their model, Mo & White (1996) obtained analytic results only in the limit of large separations (Sheth & Lemson 1999, Taruya & Suto 2000). Although not directly necessary to the development of the remaining part of the paper, I also calculate the large scale bias factor, b, in order to test the model described and to compare it with the value found by Sheth et al. (1999), as previously done with the threshold, δ_c.

In Fig. 2, I plot the bias parameter, b, as a function of the peak height ν, which is proportional to the halo mass. The solid line shows the spherical collapse prediction of Mo & White (1996), the dotted line the prediction for b obtained from our model, and the dashed line the ellipsoidal collapse prediction of Sheth et al. (1999). As shown in the figure, the effect of non-radial motions is to change the dependence of b on ν in good agreement with Sheth et al. (1999). From Fig. 2 it is evident that at the low mass end the bias relation has an upturn, meaning that less massive haloes are more strongly clustered than the prediction of the spherical collapse model of Mo & White (1996) and in agreement with N-body simulations (Jing 1998; Sheth & Lemson 1999).

2.3 PVD, CVT and non-radial motions

At this point I am ready to calculate the PVD, using the CVT in its original formulation (Peebles 1976) and the improved version of SJ97, and to study the effect of non-radial motions on these results.

Fig. 3 plots the results of the model of this paper and the comparison with the DP83 data for values of the parameter $F = 0.1, 1, 1.5$ (open squares), the IRAS value at $1h^{-1}$Mpc (filled square) (Fisher et al. 1993), the DP83 interpretation of the Turner (1976) galaxy pair catalog (solid hexagons) and the Marzke et al. (1995) data at $1h^{-1}$Mpc (dashed errorbar). ⋆ Here, the PVD, is derived using a SCDM model ($\Omega_0 = 1$, $h = 1/2$) filtered on galactic scales and normalized to $Q_{\rm COBE} = 17\mu$K. The dotted line represents the PVD obtained from the uncorrected version of the CVT.

As previously found by several authors (DP83; Mo et al. 1993; Fisher et al. 1994b; Marzke et al. 1995), the SCDM model overestimates the PVD. The dashed line represents the PVD obtained from the corrected version of the CVT (SJ97), having assumed $r_c = r_s = 10h^{-1}$kpc.

In agreement with SJ97, taking into account the finite size of galaxies reduces the small-scale velocity dispersion of galaxies, but not enough to be in agreement with observational data. The solid line represents the PVD, taking account of the non-radial motions, while the long-dashed line takes also into account the finite size of galaxies (again $r_c = r_s = 10h^{-1}$ Kpc). The finite size effect and non-radial motions both produce a decrease in the PVD. This is due to the fact that the finite size effect suppresses the effective gravitational force between pairs and changes the two-point correlation function on small scales. Non-radial motions have also the effect of changing the two-point correlation function (DG99; D99), the mass distribution and the density profile of the galactic halos (White & Zaritsky 1992; DG98). The change of mass distribution produces, in agreement with BB96, a change in the PVD predicted by the CVT, namely smaller values of the small-scale pairwise peculiar velocity dispersions of galaxies. Differently from BB96 in the model of this paper, I do not observe the rapid increase of the PVD beyond $r \simeq 1h^{-1}$Mpc with a consequent better agreement of the model with data. The difference is due to the increase of the bias parameter going from small to larger scales. Aside from the model introduced to calculate b, the behavior of the bias parameter, and then the PVD, can be qualitatively explained as follows: the papers of Sheth (1996) and Diaferio & Geller (1996) and Mo et al. (1997) suggest that, while on very small separations, pairs come from both small and large haloes, at larger separations, pairs come mainly from larger and more massive haloes. Since massive haloes have larger b values than less massive ones, this means that the effective bias is lower on small scales than on larger ones.

The CVT has been traditionally applied as an indicator of the cosmological density parameter, Ω_0, and since its first use (DP83), it was considered as a strong indicator of an open universe. Excluding the behaviour of the PVD at $r \geq 1h^{-1}$Mpc, where, as remarked by BB96, the stable clustering hypothesis could be questioned, the result of this paper is in agreement with that of BB96, namely: the PVD should not be taken as a direct evidence of a low density universe. At the light of Fig. 3, I want to add that this conclusion should be more strict if we could rely on the CVT for $r > 1h^{-1}$Mpc. At the same time, as remarked by SJ97, the usefulness of the CVT to put constraint on Ω_0 is strictly connected with the quality of the

⋆ We recall that the parameter F was introduced in the infall model used by DP83 (see DP83 equation (22)-(23)) in order to test the sensitivity of the velocity dispersion estimates to the streaming correction. According to the equation (23) in DP83, a small value of F implies that galaxies on all scales expand with the Hubble flow, while a value of $F = 1$, implies, that galaxies having separation of 5Mpc are expanding at 1/2 the Hubble rate.

[ht]

Figure 3. The PVD as a function of separation r. The PVD, is derived using a SCDM model ($\Omega_0 = 1$, $h = 1/2$), whose transfer function is given in next section, equation (26), filtered on galactic scales and normalized to $Q_{\rm COBE} = 17\mu$ K. The dotted line represents the PVD obtained from the uncorrected version of the CVT, the dashed line represents the PVD obtained from the corrected version of the CVT (SJ97) with $r_{\rm c} = r_{\rm s} = 10h^{-1}$kpc, the solid line the PVD taking into account the non-radial motions while the long-dashed line takes also into account the finite size of galaxies ($r_{\rm c} = r_{\rm s} = 10h^{-1}$kpc). The model is compared with DP83's data for values of the parameter $F = 0.1, 1, 1.5$ (open squares), the IRAS value at $1h^{-1}$Mpc (filled square) (Fisher et al. 1993), the DP83 interpretation of the Turner (1976) galaxy pair catalog (solid hexagons) and the Marzke et al. (1995) data (dashed errorbar).

observational data. In fact, as reported in the introduction, some authors (Mo et al. 1993; Marzke et al. 1995; Guzzo et al. 1997) have pointed out that the value of the PVD is very sensitive to the presence or absence of rich clusters in a sample. There is a large variation in $< v_{12}^2 >$ in different surveys and even for the same survey analyzed in different ways. Moreover, σ_{12} varies widely also because of the morphological type of the galaxies entering the catalog (Sheth et al. 2000). As shown by Mo et al. (1997), the numbers of pairs with small separations is dominated by haloes having $M \simeq M_*$ while on small scales massive pairs, $M > M_*$, strongly affect the PVD. Since the number density, n, of this massive haloes is small, a large sample is needed to have a fair sample of n or in other terms the small scale PVD can be fairly sampled only by means of samples containing many rich clusters.

3 PVD FROM DISTORTIONS IN $\xi_Z(R_{\rm P}, \pi)$

Since the combination of statistical and systematic uncertainties entering the CVT have lead several authors to conclude that it has notheworthy problems as an estimator of cosmological parameters (Fisher et al. 1994b), in order to be on the safe side, I also use a more reliable and more widely used method to estimate cosmological parameters, and in particular the PVD.

As previously reported in the introduction, the three-dimensional distribution of galaxies in redshift-space appears distorted with respect to the same distribution in real space. The correlation function measured in redshift space, $\xi(s)$, is different from the real space counterpart, $\xi(r)$, because of two effects. These effects are seen in redshift-space, plotting the correlation function in terms of two variables, the separations parallel (π) and perpendicular ($r_{\rm p}$) to the line of sight. Given a pair of galaxies with redshifts corresponding to velocities $\mathbf{v}_1$ and $\mathbf{v}_2$, the separation in redshift space is given by:

$$\mathbf{s} = \mathbf{v}_1 - \mathbf{v}_2 \tag{15}$$

while the observer's line of sight is:

$$\mathbf{l}=\frac{1}{2}(\mathbf{v}_1+\mathbf{v}_2) \tag{16}$$

The separations parallel and perpendicular to the line of sight are respectively:

$$\pi=\frac{\mathbf{sl}}{|\mathbf{l}|} \tag{17}$$

and

$$\mathbf{r}_{\rm p}^2=\mathbf{ss}-\pi^2 \tag{18}$$

The PVD can be obtained by modelling the redshift distortion of $\xi_z(r_{\rm p},\pi)$, as follows:

The statistics $\xi_z(r_{\rm p},\pi)$ is a convolution of the real-space correlation function, $\xi(r)$, with the distribution function of the relative velocity along the line of sight, $f(v_{12})$. Following, for example, Fisher et al. 1994b, Jing & Börner (1998) (hereafter JB98), we have:

$$1+\xi_z(r_{\rm p},\pi)=\int f(v_{12})\left[1+\xi\left(\sqrt{r_{\rm p}^2+(\pi-v_{12}/H_0)^2}\right)\right]dv_{12} \tag{19}$$

To obtain the PVD from $\xi_z(r_{\rm p},\pi)$ there are at least three methods (Peebles 1980, section 76). The first one, which I am going to use in this paper and which is the more diffused in papers that try to recover the PVD from survey of galaxy redshift (Davis & Peebles 1983; Mo et al. 1993; J98; JB98), can be summarized in the following steps:
1) Estimate of the redshift-space two-point correlation function $\xi_z(r_{\rm p},\pi)$. If one has observational data, coming from a redshift survey, it is necessary to choose an estimator for $\xi_z(r_{\rm p},\pi)$ (see for example J98). In our case, $\xi_z(r_{\rm p},\pi)$ is to be calculated theoretically from the power spectrum, as I am going to do.
2) Estimate of the projected two-point correlation function $w(r_{\rm p})$:

$$w(r_{\rm p})=2\int_0^\infty \xi_{\rm z}(r_{\rm p},\pi)d\pi=2\int_0^\infty \xi(\sqrt{r_{\rm p}^2+y^2})dy \tag{20}$$

3) Calculation of the two-point correlation function $\xi(r)$.
4) Assumption of a functional form for $f(v_{12})$, an infall model for $\overline{v}_{12}$ to, finally, solve equation (19) for σ_{12}.

For seek of completeness, I shortly describe the other two methods. The second approach follows from Eq. 19. After determining $\xi(r)$ from:

$$\int_0^\infty \xi_{\rm z}(r_{\rm p},\pi)=\int_0^\infty \xi(\sqrt{r_{\rm p}^2+y^2})dy \tag{21}$$

the PVD can be obtained by the equation:

$$<v_{12}^2>=3H_0^2\int_0^\infty d\pi\pi^2\left[\xi_{\rm z}(r_{\rm p},\pi)-\xi(\sqrt{r_{\rm p}^2+y^2})\right]/\int_0^\infty \xi_{\rm z}(r_{\rm p},\pi)d\pi \tag{22}$$

(see also Peebles 1979). This method does not require the knowledge of $f(v_{12})$ but, as noted by Davis & Peebles (1983), the integral depends sensitively on ξ at $|\pi|\geq 1000$km/s, where, if one uses data from redshift surveys, $\xi_{\rm z}(r_{\rm p},\pi)$ is poorly known. The third method also deriving from Eq. 19 is:

$$<v_{12}^2>=3H_0^2\int_0^\infty d\pi dr_{\rm p}(\pi^2-r_{\rm p})\xi_{\rm z}(r_{\rm p},\pi)/\int_0^\infty \xi_{\rm z}(r_{\rm p},\pi)d\pi dr_{\rm p} \tag{23}$$

which requires only $\xi_{\rm z}(r_{\rm p},\pi)$ but also this approach, as the previous one, is not free from drawbacks (see Peebles 1980, Sect. 76).
Coming back to the first method, we can start from the step (1).

In order to get $\xi_{\rm z}(r_{\rm p},\pi)$, I Fourier transform the redshift-space power spectrum:

$$\xi(s,\mu_{\mathbf{sl}})^S=\frac{1}{(2\pi)^3}\int d^3\mathbf{k}P^S(k,\mu_{\mathbf{kl}})\exp\left(-iks\mu_{\mathbf{ks}}\right) \tag{24}$$

(see Cole et al. 1994, equation (B1)), where, as previously quoted, $\mathbf{l}$ denotes the direction of the line of sight, $\mu_{\mathbf{ks}}$ and $\mu_{\mathbf{kl}}=\frac{k_\parallel}{(k_\parallel^2+k_\perp)^{1/2}}$ the cosine between the vectors $\mathbf{s}$, $\mathbf{k}$ and $\mathbf{k}$, $\mathbf{l}$, respectively ($k_\perp$ and $k_\parallel$ are the components of the wavevector perpendicular and parallel to the line of sight). $\xi_{\rm z}(r_{\rm p},\pi)$ can be obtained from equation (24) by changing variables according to equation (15)-(18).

Before going on, I want to recall that there are three effects that cause a departure of the observed clustering properties of galaxies from the linear spectrum:
a) Redshift space effects. We extract three dimensional clustering information from redshift surveys; in these surveys, the galaxy radial coordinates are distorted by peculiar velocities.

b) Nonlinear evolution, producing, on small scales, a departure of the mass spectrum from its initial form.
c) Bias. Different classes of objects trace mass in different ways leading to difficulties in connecting theory and observations.

Firstly, (relatively to point a), in order to calculate the redshift space power spectrum, distorted by the peculiar velocity field, I use the expression given by Peacock & Dodds (1994) and Cole et al. (1995):

$$P^S(k_\perp, k_\parallel) = P^R(k)\left[1+\beta\mu_{\mathbf{kl}}^2\right]^2\left(1+k^2\sigma_{12}^2\mu_{\mathbf{kl}}^2/2\right)^{-2} \tag{25}$$

where $k=\sqrt{k_\parallel^2+k_\perp^2}$, $P^R(k)$ is the real-space power spectrum, and $\beta=\frac{f(\Omega)}{b}$, where the perturbation parameter $f(\Omega)$ is defined in Peebles 1980 (section 14). The real-space power spectrum that I adopt is $P(k)=AkT^2(k)$ with the transfer function $T(k)$ given in BBKS (equation (G3)):

$$T(k)=\frac{[\ln(1+2.34q)]}{2.34q}\cdot[1+3.89q+(16.1q)^2+(5.46q)^3+(6.71)^4]^{-1/4} \tag{26}$$

where A is the normalizing constant and $q=\frac{k\theta^{1/2}}{\Omega_X h^2\mathrm{Mpc}^{-1}}$. Here $\theta=\rho_{\mathrm{er}}/(1.68\rho_\gamma)$ represents the ratio of the energy density in relativistic particles to that in photons ($\theta=1$ corresponds to photons and three flavors of relativistic neutrinos). The power spectrum was COBE normalized using the cosmic microwave anisotropy quadrupole $Q_{rms-PS}=17\mu\mathrm{K}$ that corresponds to $\sigma_8=0.95\pm0.2$ (Smoot et al. 1992; Liddle & Lyth 1993).

Secondly, (relatively to point b), since I have to calculate the PVD in the range $0.01\le r_{\mathrm{p}}\le 10h^{-1}\mathrm{Mpc}$ I should take into account the non-linear evolution of the power spectrum.

To this aim, I shall use the fitting formula of Peacock & Dodds (1996) (see also Hamilton et al. (1991), Peacock & Dodds (1994), Jain et al. (1995), Mo et al. (1997)), relating the evolved power variance, $\Delta_{\mathrm{E}}^2=\frac{1}{2\pi^2}k^3P(k)_E$, to the initial density spectrum:

$$\Delta_{\mathrm{E}}^2(k_{\mathrm{E}})=F([\Delta^2(k_{\mathrm{L}})]) \tag{27}$$

where L stands for 'linear' E for 'evolved', $k_{\mathrm{L}}=[1+\Delta_{\mathrm{E}}^2(k_{\mathrm{E}})]^{-1/3}k_{\mathrm{E}}$ and the functional form of F is given in Peacock & Dodds (1996). This correction was done to the real-space spectrum in equation (25) which shall be introduced in equation (24) to obtain $\xi_{\mathrm{z}}(r_{\mathrm{p}},\pi)$.

After $\xi_z(r_{\mathrm{p}},\pi)$ has been calculated, we can go to step (2) and (3).

Following the usual technique used to recover the real-space correlation function from $\xi_z(r_{\mathrm{p}},\pi)$, I define a projected function $w(r_{\mathrm{p}})$, unaffected by redshift distortions:

$$w(r_{\mathrm{p}})=2\int_0^\infty\xi_{\mathrm{z}}(r_{\mathrm{p}},\pi)d\pi=2\int_0^\infty\xi(\sqrt{r_{\mathrm{p}}^2+y^2})dy \tag{28}$$

(DP83). Then $\xi(r)$ can be obtained, following DP83, either solving $w(r_{\mathrm{p}})$ for $\xi(r)$, or also fitting $w(r_{\mathrm{p}})$ to a power law model for $\xi(r)$. Following the first alternative $\xi(r)$ is given by evaluating the Abel integral:

$$\xi(r)=-\frac{1}{\pi}\int_r^\infty dr_{\mathrm{p}}w(r_{\mathrm{p}})(r_{\mathrm{p}}^2-r^2)^{-1/2} \tag{29}$$

(DP83) (an alternative method to calculate $\xi(r)$, even if more complex, and compatible with that previously presented, as remarked by Peebles (1983) and J98, should be that presented in D99, and based on the use of the Limber's equation. As shown in that case, the effect of non-radial motions is that of producing enough additional clustering to fit the $\xi(r)$ of the APM galaxy survey).

Finally, (step 4), I need a functional form for $f(v_{12})$. A good approximation to this function is:

$$f(v_{12})=\frac{1}{\sqrt{2}\sigma_{12}}\exp\left(-\frac{\sqrt{2}|v_{12}-\overline{v}_{12}|}{\sigma_{12}}\right) \tag{30}$$

(Fisher et al. 1994b; J98), where $\overline{v}_{12}$ and σ_{12} are the mean and the dispersion of the 1-D pairwise peculiar velocities. The infall, $\overline{v}_{12}$, is difficult to model because it is correlated with σ_{12}, and it is scale dependent. Following J98, I assume a self-similar infall model for $\overline{v}_{12}$:

$$\overline{v}_{12}(\mathbf{r})=\frac{-yH_0}{1+(r/r_*)^2} \tag{31}$$

where $r_*=5h^{-1}\mathrm{Mpc}$ and y is the radial separation in real space. This infall model is usually assumed, because it gives a good approximation to the infall pattern seen in CDM models and, as shown, in JB98, J98 the PVD reconstructed using this model is in good agreement with the 3-D velocities in the simulations.

As stressed by J98, the method described to determine the PVD is approximated for several reasons:
1) the functional forms of $f(v_{12})$ and $v_{12}(r)$ are approximations;

[ht]

Figure 4. The PVD calculated from the redshift-space distortion of $\xi_{\rm z}(r_{\rm p},\pi)$. The solid line is the PVD taking account of non-radial motions, the dashed line the PVD obtained from the SCDM model that does not take account of the non-radial motions. The data are the PVD measured from the Las Campanas Redshift Survey by J98.

2) the reconstruction of the PVD from redshift distortion gives, as a result, only an average of the real PVD along the line of sight.
In any case, the value of σ_{12}, obtained with the quoted technique, is within 20% of the true PVD (JB98).

At this stage, I have all the quantities required by equation (19) to obtain $\xi_z(r_{\rm p},\pi)$. I have obtained the PVD by using equation (19) and fitting σ_{12} to $\xi_{\rm z}(r_{\rm p},\pi)$ (see Peebles 1980; DP83; Mo et al. 1993; J98). The calculation was repeated two times, the first with $\delta_{\rm c}=1.686$ and the second assuming equation (8).
The result of the model described in this section is shown in Fig. 4. Here the solid line represents the PVD, taking into account non-radial motions, the dashed line the PVD obtained from the SCDM model that does not take into account the non-radial motions. The theoretical results are compared with the PVD measured from the Las Campanas Redshift Survey by J98. As shown in Fig. 4, the PVD predicted by the SCDM model that does not take into account non-radial motions is higher than the observed value for all $r_{\rm p}$ except at $r_{\rm p}=30h^{-1}$Mpc. However, as pointed out by J98, the results on scales larger than $5h^{-1}$Mpc are very sensitive to the model for the infall chosen, since the statistical fluctuations become very large. The result confirms the well known limit of the CDM model to reproduce the two-point correlation function, to which the PVD is connected, since it probes the clustering power on small scales. As stressed several times, the discrepancy of the $\xi(r)$ on scales $r_{\rm p}\geq 5h^{-1}$Mpc is due to the fact that this model does not have enough power on large scales. Unless the PVD of galaxies is biased relative to that of the mass, the CDM model have problems in fitting the observed data. Moreover, using a constant bias, it is possible to fit the data only on a limited radius range. Fig. 4 shows that the introduction of a scale-dependent bias, due to non-radial motions, produces a notheworthy reduction of the discrepancy of the PVD measured from the Las Campanas Redshift Survey with respect to the prediction of the CDM model. The mechanism giving rise to this bias was described in the previous section and more widely in DG98, DG99, DG00, D99. Before concluding, it is interesting to note that, J98, showed that a scale-dependent bias may explain the discrepancy between the model predictions and observational results. In agreement with J98, a velocity bias is not needed to make models compatible with the observed PVD.

4 CONCLUSIONS

In this paper, I have studied the effect of non-radial motions on the PVD in a SCDM model extending the model introduced in DG98 and D99. Firstly, I calculated the effect of non-radial motions on the threshold $\delta_{\rm c}$ and bias. I then compared the large scale bias, calculated by means of the model of this paper, with the prediction of Mo & White (1996) model for a spherical collapse model and with the result of Sheth et al. (1999) for an ellipsoidal collapse, finding a good agreement with the result of this last paper. The model for the bias was used in the SJ97 improved version of CVT to determine the PVD, which was compared with the data from DP83, the IRAS value at $1h^{-1}$Mpc of Fisher et al. (1993) and Marzke et al. (1995). As shown in Fig. 3, non-radial motions produce a reduction of the values of the PVD, with respect to the prediction of a SCDM model that does not take into account this effect. The result is due to the scale-dependent non-local bias induced by non-radial motions and to the change of mass distribution in galactic halos. At the light of BB96, the result may be also read as a strong dependence of the CVT prediction on the model chosen to describe the mass distribution around galaxies, suggesting that the CVT cannot be taken as a direct evidence of a low density universe.

Finally, I calculated the PVD by means of the redshift distortion in the redshift-space correlation function, $\xi_{\rm z}(r_{\rm p}, \pi)$, and compared it with the data obtained by J98 from the Las Campanas Redshift Survey. The result confirmed that non-radial motions reduce the discrepancy between SCDM model predictions and observations.

ACKNOWLEDGEMENTS

I would like to thank Y.P. Jing, R. Sheth, A. Diaferio and E. Nihal Ercan for some useful comments that helped me in improving this paper. Finally, I would like to thank Bo*ğazi*çi University Research Foundation for the financial support through the project code 01B304.

REFERENCES

Audit E., Teyssier R., Alimi J. M., 1997, A&A, 325, 439
Bardeen J.M., Bond J.R., Kaiser N., Szalay A.S., 1986, ApJ, 304, 15
Bartlett J.G., Blanchard A., 1996, A&A 307, 1
Bean A.J., Efstathiou G.P., Ellis R.S., Peterson B.A., Shanks T., 1983, MNRAS, 205, 605
Borgani S., 1990, A&A 240, 223
Colafrancesco S., Antonuccio V., Del Popolo A., ApJ, 1995, 455, 32.
Cole S., Fisher K. B., Weinberg D., 1994, MNRAS, 267, 785
Cole S., Fisher K.B., Weinberg D.H., 1995, MNRAS, 275, 515
Davis M., Geller M.J., Huchra J., 1978, ApJ, 221, 1
Davis M., Peebles P.J.E., 1983, ApJ, 267, 465
Del Popolo, A., Gambera, M, 1998, A&A, 337, 96
Del Popolo A., Gambera M., 1999, A&A, 344, 17
Del Popolo A., Takahashi Y., Kiuchi H., Gambera M., 1999, A&A, 348, 667
Del Popolo A., Gambera M., 2000, A&A, 357, 809
Del Popolo A., Gambera M., Spedicato E., Recami E., 2000, A&A, 353, 427.
Diaferio A., Geller M. J., 1996, ApJ, 467, 19
Fisher K.B., Davis M., Strauss, M.A., Yahil A., Huchra J.P., 1993, MNRAS, 266, 50
Fisher K.B., Davis M., Strauss, M.A., Yahil A., Huchra J.P., 1994a, MNRAS, 266, 50
Fisher K.B., Davis M., Strauss, M.A., Yahil A., Huchra J.P., 1994b, MNRAS, 267, 927
Groth, E.J., Peebles P.J.E., 1977, ApJ, 217, 385
Guzzo L., Strauss M.A., Fisher K.B., Giovanelli R., Haynes M.P., 1997, ApJ, 489, 37
Jain B., Mo H. J., White S. D. M., 1995, MNRAS, 276, L25
Jing Y.P., Mo H.J., Börner G., 1998, ApJ, 494, 1
Jing Y.P., Börner G., 1998, ApJ, 503, 502
Jing Y., 1998, ApJL, 503, L9
Jing, Y. P., Börner G., Suto Y., preprint Sissa astro-ph/0104023
Kaiser, N., 1984, ApJ, 284, L9
Hamilton A. J. S., Kumar P., Lu E., Matthews A., 1991, ApJ, 374, L1
Hoffman Y., 1986, ApJ, 301, 65
Liddle A.R., Lyth D.H., 1993, Phys. Rep., 231, n 1, 2
Lilje P.B., Lahav O., 1991, ApJ, 374, 29
Lin H., 1995, Ph.D. Thesis, Harvard University
Magira H., Jing Y.P., Suto Y., 2000, ApJ, 528, 30
Marzke R.O., Geller M.J., da Costa L.N., Huchra J.P., 1995, AJ, 110, 477
Mo H.J., Jing Y.P., Börner G., 1993, MNRAS, 264, 825
Mo H.J., White S.D.M., 1996, MNRAS, 282, 347
Mo H.J., Jing Y.P., Börner G., 1997, MNRAS, 286, 979

Peacock J.A., Dodds S.J., 1994, MNRAS, 267, 1020
Peacock J.A., Dodds S.J., 1996, MNRAS, 280, L19
Peebles P.J.E., 1976, Astrophys.Sp.Sci., 45, 3
Peebles P.J.E., 1979, AJ, 84, 730
Peebles P.J.E., 1980, The large scale structure of the Universe, Princeton university press
Peebles P.J.E., 1990, ApJ 365, 27
Ryden B.S., Gunn J.E., 1987, ApJ, 318, 15
Ryden B.S., 1988, ApJ, 333, 78
Sheth R.K., 1996, MNRAS, 281, 1277
Sheth R.K., Lemson G., 1999, MNRAS, 304, 767
Sheth R.K., Mo H.J., Tormen G., 1999, preprint SISSA astro-ph/9907024
Sheth R.K., Diaferio A., Hui L., Scoccimarro R., 2000, preprint SISSA astro-ph/0010137
Smoot G.F., et al., 1992, ApJ, 396, L1
Strauss M.A., 1997, Redshift Surveys of the Local Universe, in Formation of Structure in the Universe, edited by A. Dekel and J. Ostriker (Cambridge: Cambridge University Press)
Suto Y., 1993, Prog. Theor. Phys., 90, 1173
Suto Y., 1996, astro-ph-9609014
Suto Y., Jing, Y.P., 1997, ApJS, 110, 167
Taruya A., Suto Y., 2000, preprint SISSA astro-ph/0004288
Turner E.L., 1976, ApJ, 208, 20
White, S. D. M., Zaritsky, D., 1992, ApJ, 394, 1

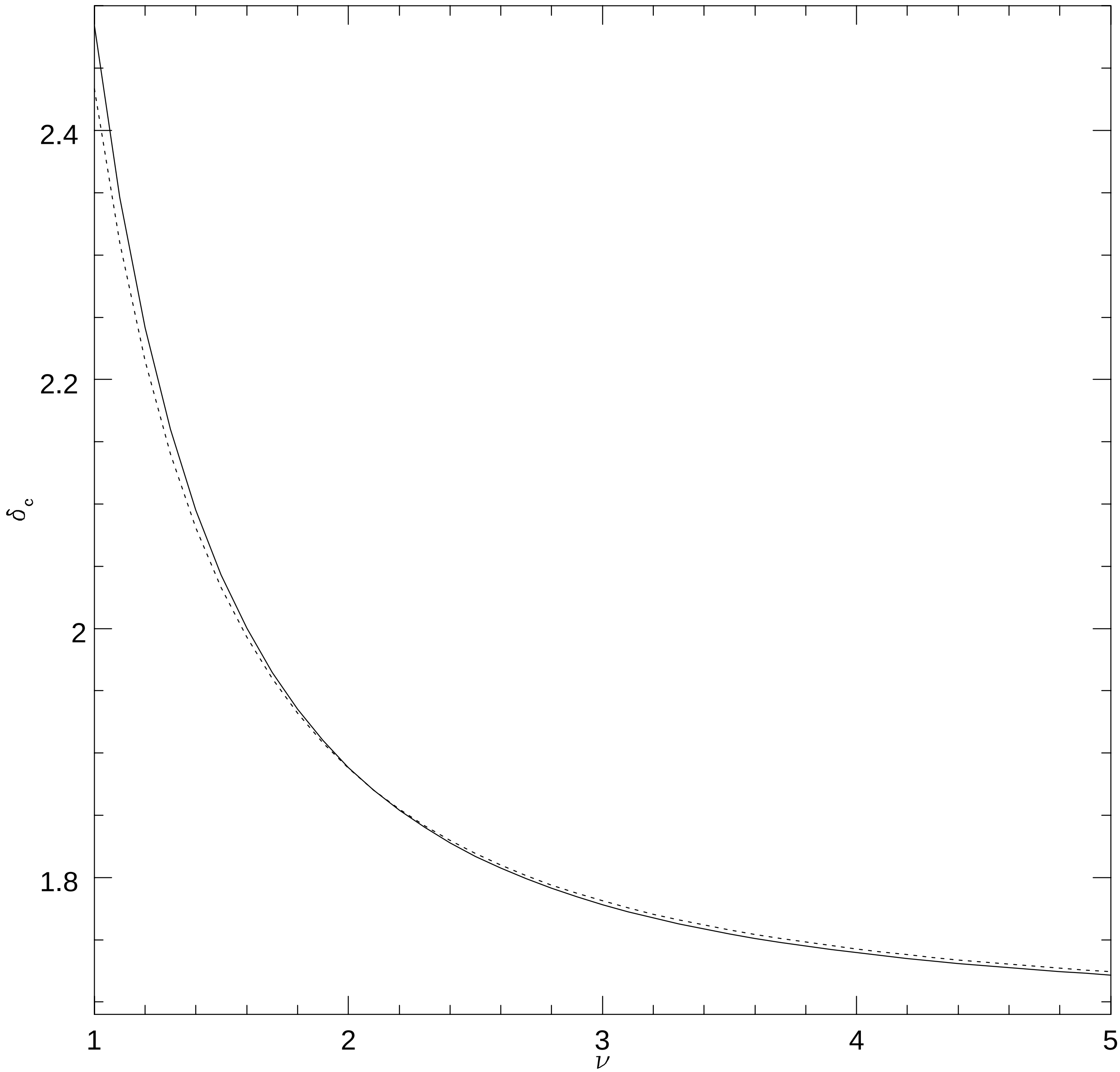
2.4
2.2
2
1.8
δ_c
1
2
3
4
5
ν

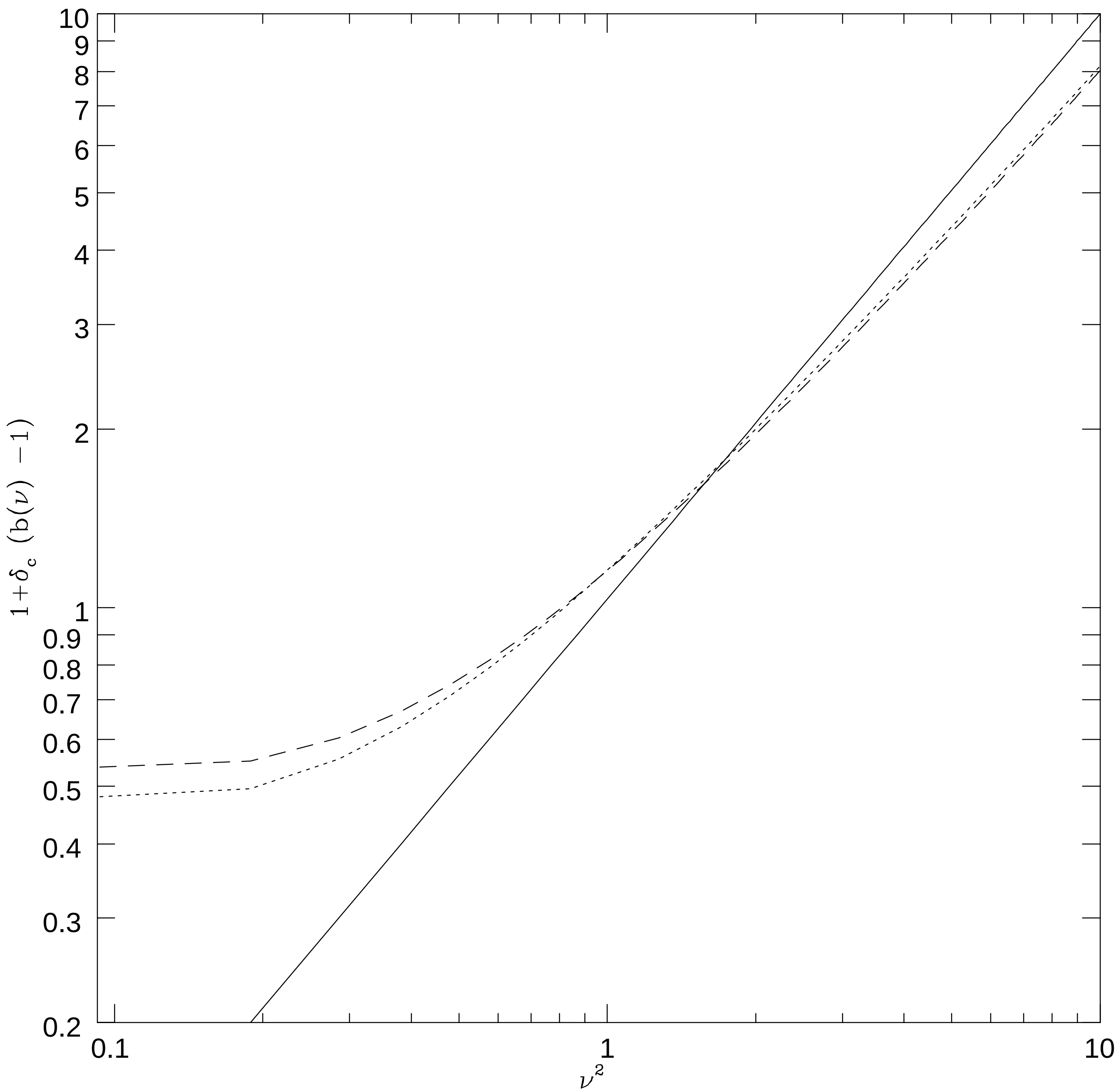

10
9
8
7
6
5
4
3
2
1
0.9
0.8
0.7
0.6
0.5
0.4
0.3
0.2
$1+\delta_c\ (b(\nu)\ -1)$
0.1
1
10
ν^2

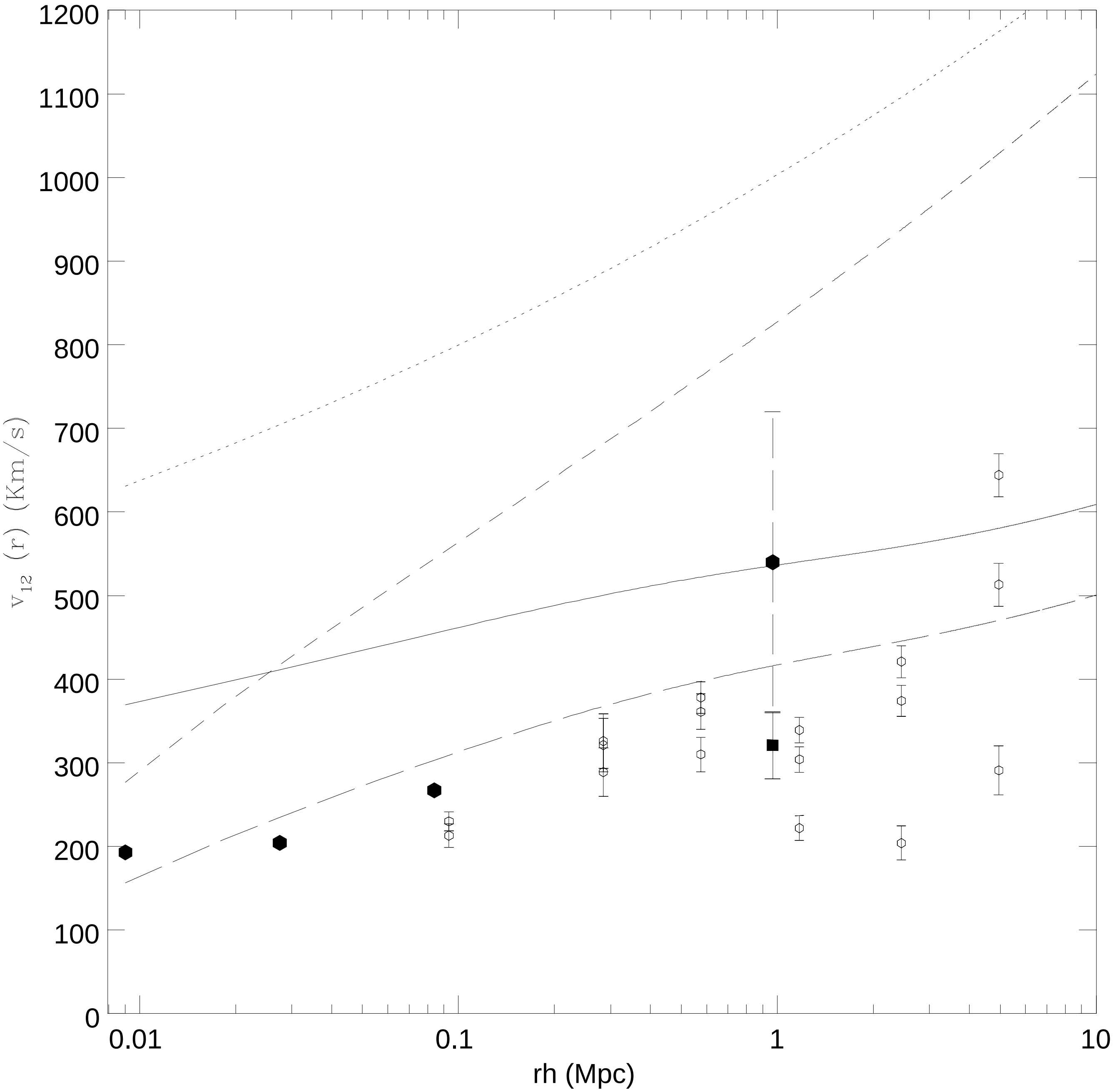

1200
1100
1000
900
800
700
600
500
400
300
200
100
0
v_{12} (r) (Km/s)
0.01
0.1
1
10
rh (Mpc)

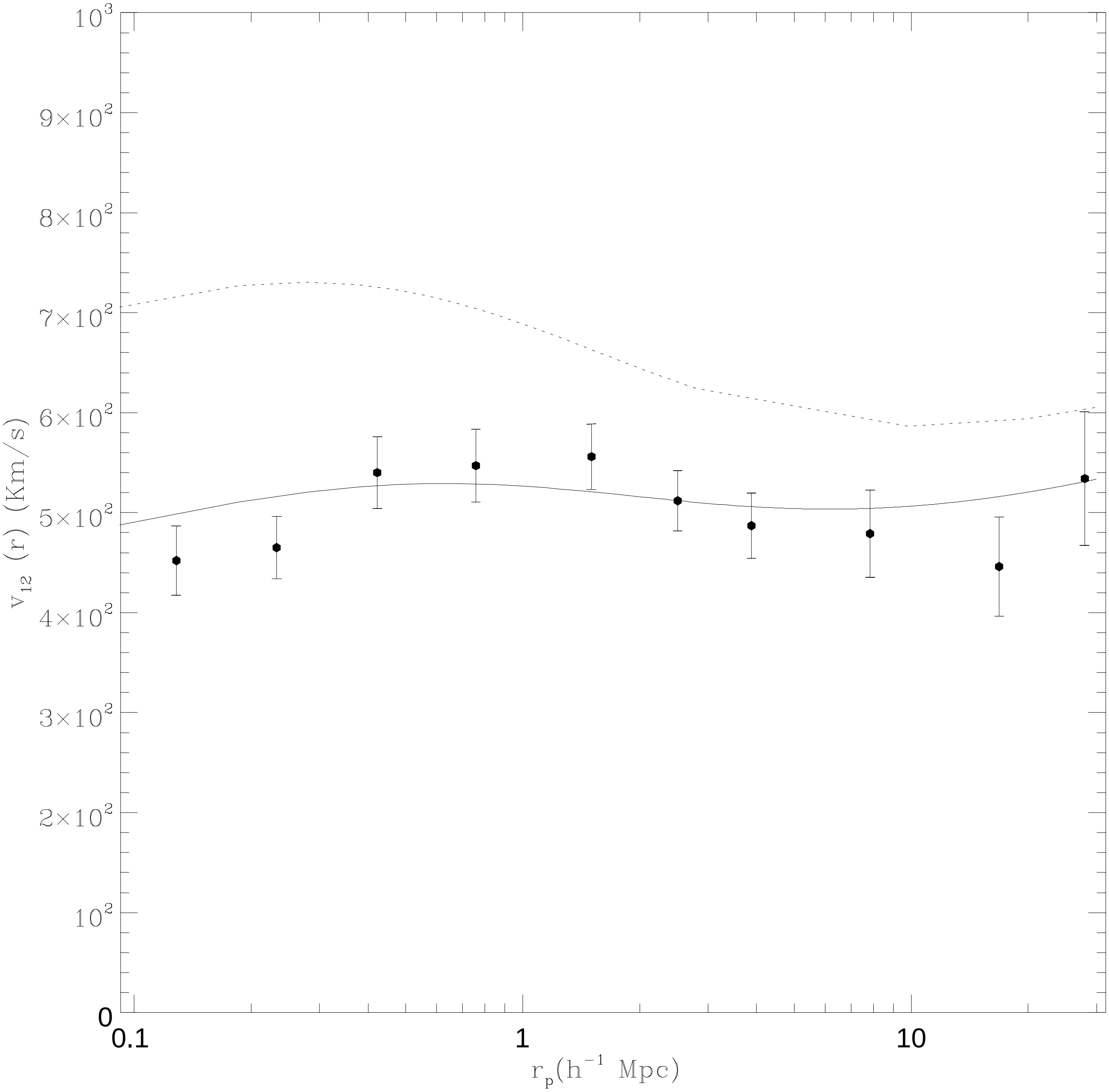

10^3
9×10^2
8×10^2
7×10^2
6×10^2
5×10^2
4×10^2
3×10^2
2×10^2
10^2
0
v_{12} (r) (Km/s)
0.1
1
10
$r_p(h^{-1}$ Mpc)